ORIGINAL ARTICLE

Rotors Detected by Phase Analysis of Filtered, Epicardial Atrial Fibrillation Electrograms Colocalize With Regions of Conduction Block

BACKGROUND: Several recent studies suggest rotors detected by phase mapping may act as main drivers of persistent atrial fibrillation. However, the electrophysiological nature of detected rotors remains unclear. We performed a direct, 1:1 comparison between phase and activation time mapping in high-density, epicardial, direct-contact mapping files of human atrial fibrillation.

METHODS: Thirty-eight unipolar electrogram files of 10 s duration were recorded in patients with atrial fibrillation (n=20 patients) using a 16×16 electrode array placed on the epicardial surface of the left atrial posterior wall or the right atrial free wall. Phase maps and isochrone wave maps were constructed for all recordings. For each detected phase singularity (PS) with a lifespan of >1 cycle length, the corresponding conduction pattern was investigated in the isochrone wave maps.

RESULTS: When using sinusoidal recomposition and Hilbert Transform, 138 PSs were detected. One hundred and four out of 138 PSs were detected within 1 electrode distance (1.5 mm) from a line of conduction block between nonrotating wavefronts detected by activation mapping. Far fewer rotating wavefronts were detected when rotating activity was identified based on wave mapping (18 out of 8219 detected waves). Fourteen out of these 18 cases were detected as PSs in phase mapping. Phase analysis of filtered electrograms produced by simulated wavefronts separated by conduction block also identified PSs on the line of conduction block.

CONCLUSIONS: PSs identified by phase analysis of filtered epicardial electrograms colocalize with conduction block lines identified by activation mapping. Detection of PSs using phase analysis has a low specificity for identifying rotating wavefronts during human atrial fibrillation using activation mapping.

VISUAL OVERVIEW: A visual overview is available for this article.

Piotr Podziemski, PhD*
Stef Zeemering, PhD*
Pawel Kuklik, PhD
Arne van Hunnik, BSc
Bart Maesen, MD, PhD
Jos Maessen, MD, PhD
Harry J. Crijns, MD, PhD
Sander Verheule, PhD
Ulrich Schotten, MD, PhD

WHAT IS KNOWN?

- Several recent studies suggest rotors detected by phase mapping may act as main drivers of persistent atrial fibrillation.
- The electrophysiological nature of detected rotors remains unclear.

WHAT THE STUDY ADDS?

- Phase singularities identified by phase analysis of filtered epicardial electrograms colocalize with conduction block lines identified by activation mapping but have low specificity for identifying rotating wavefronts during human atrial fibrillation.
- Phase analysis of filtered electrograms produced by simulated wavefronts separated by conduction block also identified phase singularities on the line of conduction block.
- These findings were reproducible after using a variety of methods for (1) activation time annotation of fibrillation electrograms, (2) filtering of epicardial electrograms, and (3) phase analysis of epicardial electrograms.

Atrial fibrillation (AF) is the most common sustained arrhythmia in adults and associated with substantial morbidity and lower quality of life.[1] Catheter ablation has been developed to eliminate sites or regions triggering AF. Although in patients with paroxysmal AF, pulmonary vein isolation shows satisfactory efficacy,[2] the results are less convincing in patients with persistent AF, possibly because the driver mechanisms are more diverse and not restricted to the pulmonary vein area.[3–5]

The current plethora of proposed mechanisms sustaining AF may partially reflect the different techniques applied to map the arrhythmia. Traditionally, multiple wavelets, randomly interacting with each other and thereby continuously resulting in new wavefront generation were believed to underlie AF.[6,7] The hypothesis was supported by the notion of multiple, simultaneous AF wavefronts using high-density direct-contact mapping[8,9] or ECG-Imaging (ECG-I, a noninvasive technique based on phase analysis of body surface potentials).[10,11] More recently, several groups have advocated localized rotating drivers perpetuating AF in humans. Using phase analysis of endocardial atrial electrograms recorded with a basket catheter, Narayan et al[12] introduced Focal Impulse and Rotor Modulation (FIRM), a technology capable of identifying localized rotors as sources of AF. When the cores of these rotors were ablated, AF often terminated.[13,14] Early meta-analyses showed benefit of driver-guided ablation for AF,[15] but subsequent meta-analyses have been more conflicting.[16,17] Haissaguerre et al[11] also detected rotors but used ECG-I instead of direct-contact mapping. Also in this study, ablation of areas where the cores of the rotors preferentially occurred could terminate AF in a large proportion of patients.

All methods mentioned above require various degrees of preprocessing of recorded electrograms. Wave mapping of direct-contact electrograms offers very detailed analysis of fibrillation patterns but requires annotation of local activation times based on electrogram deflections. This strenuous work traditionally has been performed manually but was recently automated.[9,18] Noninvasive ECG-I requires a solution to the ill-posed inverse problem and regularization of the results. Importantly, both ECG-I and FIRM basket mapping use phase analysis of electrograms to determine conduction behavior during AF.

Phase mapping of fibrillation electrograms requires prefiltering of the signals—as a consequence—fibrillatory patterns determined using phase analysis both in ECG-I[10] and FIRM[12,19] show a higher spatial organization and a much lower complexity than those determined using high-density contact mapping of local activation times potentially leading to misinterpretation of electrophysiological phenomena. Here, we provide a direct, 1:1 comparison of phase mapping of filtered electrograms and activation time mapping based on a high-density contact mapping dataset.

METHODS

The authors agree to make available the data in anonymised form (unless legally restricted), methods used in the analysis, and materials used to conduct research for joint analyses on request.

Electrophysiological Study

Each patient provided a written informed consent to the study protocol, which had been approved by the Institutional Ethics Committee (METC [Medisch Ethische Toetsingscommissie] Maastricht University). Intraoperative epicardial, direct-contact mapping was performed in 20 patients (11 in paroxysmal AF, 9 in persistent AF) undergoing open-chest surgery using an electrode array of 16×16 electrodes with an interelectrode distance of 1.5 mm (single-use, custom-made, gold-coated electrode array). Patient characteristics are presented in Table I in the Data Supplement. The electrode array was positioned on the left atrial posterior wall between the pulmonary veins or on the right atrial free wall, as depicted in Figure 1A. A silver plate was placed in the thoracic cavity and served as a reference electrode. Atria were mapped sequentially for 10 s at each site using a 256-channel mapping amplifier (bandwidth, 0.56–408 Hz; sampling rate, 1 kHz, resolution 12 bits). Far-field QRS complexes were subtracted from the fibrillation electrograms by single beat cancelation method.[18] After exclusion of poor contact recordings (<5% of all signals), 38 recordings were included (18 in left atrium and 20 in right atrium).
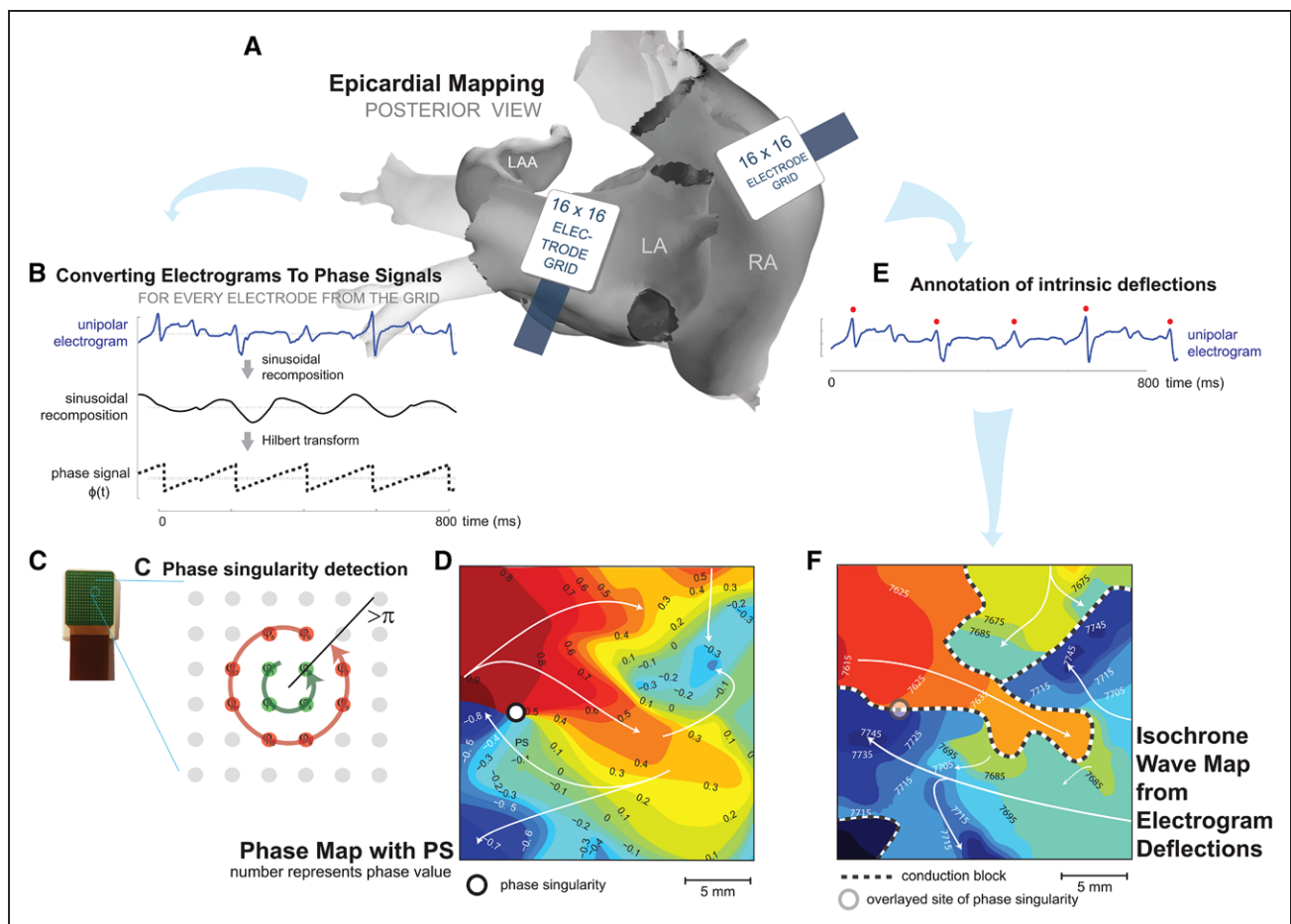
Figure 1. Epicardial mapping of right atrium (RA) and left atrium (LA).
A, High-density electrode arrays—16×16 electrodes with 1.5 mm intraelectrode distance. **B**, Phase signal obtained from unipolar electrograms through sinusoidal recomposition (middle signal) and Hilbert transform (bottom signal).[20] **C**, A phase singularity (PS) is detected if phase differences are greater than π in any 2×2 ($\varphi_1 \div \varphi_4$) and 4×4 ($\varphi_5 \div \varphi_{12}$) electrode rings.[21] **D**, Phase map achieved from sinusoidal recomposition and Hilbert transform. **E**, Example of unipolar electrograms were processed to calculate activation times (red dots above electrogram). **F**, Example of an isochrone wave map achieved by intrinsic activation detection from unipolar electrograms. LAA indicates left atrial appendage.

Activation Mapping and Conduction Block Detection

Local atrial activations were detected and annotated in the unipolar electrograms using a probabilistic algorithm described previously.[18] Briefly, local candidate deflections were detected using template matching. A probability density function of the AF cycle length (CL) was calculated based on the largest and steepest candidate deflections. Candidate deflections were subsequently assigned to groups of true local activations or subsidiary deflections (eg, deflections because of far-field or fragmented activations) so that the match of the AF CL histogram and the calculated probability density function was maximal.[18]

To compare results of automatic activation time annotation with another method, a subset of the recording was annotated manually (section 2.5 in the Data Supplement).

Isochrone wave maps were constructed based on the local activation times, as described previously.[9,22] Waves were defined as groups of electrode activations interconnected by normal conduction (CV≥CV_{block}, where CV indicates conduction velocity) and separated by lines of conduction block, marked on the isochrone wave maps as a dashed line. Waves of <3 electrodes were excluded from analysis. Waves were classified as rotating if their wavefront followed a self-intersecting path of normal conduction that lasted for >75% of the median AF CL.

Conduction block between 2 adjacent electrodes was defined as a local activation time difference corresponding a local conduction velocity below a threshold value (default CV_{block}=10 cm/s, if not stated otherwise in the article). The duration of conduction block between a pair of electrodes was measured as the time from the appearance of local conduction block until the next incidence of normal conduction. Intrawave blocks were not taken into consideration, as such blocks may appear as a result of a drift or meandering of functional reentry pivot points (See Data Supplement for further discussion). In the article, by conduction block, we understand a line of conduction block that separates 2 waves that did not have a viable conductive connection anywhere in the field of view of electrode array.

To check how rotating wavefronts in activation time mapping relate to detected phase singularities (PSs) in phase mapping, we compared the location of geometric center of rotating waves with PS locations.
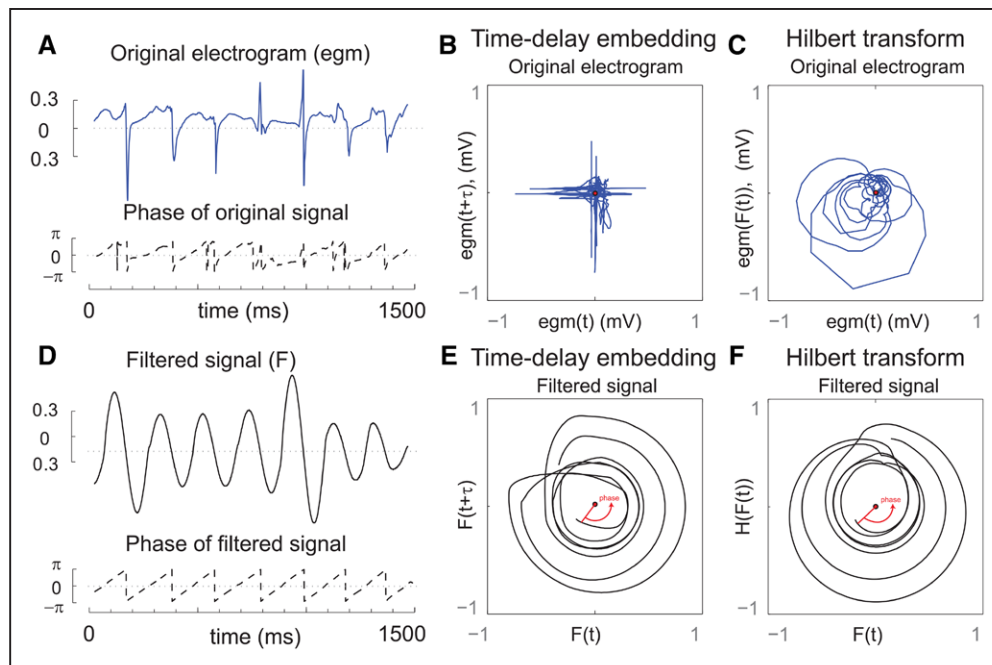
Figure 2. Techniques of reconstructing phase of an atrial electrogram.
A, A 1500 ms segment of an atrial electrogram (egm) with low fractionation (upper signal) and the corresponding phase (lower signal). Applying phase reconstruction by time-delay embedding or Hilbert transform directly on nonfiltered signal produces more phase transitions in the phase signal than actual activations in the egm signal. Reconstruction of phase trajectory in phase space is depicted in **B** for time-delay embedding and **C** for Hilbert transform. Without preprocessing the signal, the trajectory does not visibly rotate around the center, and phase cannot be properly defined. **D**, Atrial egm after filtering by sinusoidal recomposition and corresponding phase derived from filtered signal. Phase state plots of time-delay embedding (**E**) and Hilbert transform (**F**) show smooth circular trajectories for which the phase angle can be well defined. H(F(t)) indicates Hilbert transform of function F(t).

Phase Mapping

The first step of phase mapping is the calculation of electrogram phase. If phase reconstruction methods are directly applied on unfiltered atrial electrograms, the phase signal shows frequent phase transitions caused by fractionation and complex morphology of the signals as presented in Figure 2A–2C. To avoid frequent phase transitions unrelated to the activation cycles, appropriate filtering must be performed before phase calculation.

In this study, we compared 2 filtering methods. As the main method, we applied the concept of sinusoidal recomposition which, combined with the Hilbert transform, was demonstrated to reconstruct electrogram phase in a robust way, as presented in Figure 2D–2F.[20,23] In parallel, we applied a recently published filtering method[24] that is based on previous studies applying filtering in frequency domain to facilitate identification of electrogram deflections during AF.[25–27] This filtering technique extracts a smooth signal proportional to the energy present in the deflection reflecting local activations, present in the high-frequency band (40–250 Hz).[27]

To reconstruct phase from a filtered signal, we compared 2 methods, the Hilbert transform[20,23] and time-delay embedding.[28,29] Time-delay embedding reconstructs a trajectory in phase state space by plotting a signal against the same signal delayed by time τ allowing for assigning a phase angle (or phase) to the current sample of the measured signal. Time-delay τ was taken as 0.25 of the local AF CL as suggested earlier.[28,29]

In the next step, PSs were detected using calculated phase signals. Several different approaches to identify PSs have been suggested in the past.[21,28,30,31] Here, a PS was defined as a point around which a gradual phase increase followed by a phase transition $>\pi$ was present.[23] To increase robustness of PS detection, we tested whether the criterion mentioned above was met in 2 paths encircling the tested point (Figure 1C, electrodes marked by red dots). One circle is formed by electrodes at 1.5 mm distance (2×2 grid) and 1 formed by electrodes 3 mm from the tested point (outer, 4×4 grid). For full explanation, see the Data Supplement or Kuklik et al.[23] A PS was included into analysis if the PS lifespan was greater than the local AF CL. Local AF CL was defined as average interval between consecutive local deflections in all of the neighboring electrodes. In this article, only PSs with a life span of at least 1 rotation were taken into consideration.

Spatial Comparison Between Conduction Block Lines and Phase Singularity

At the moment of PS detection, we compared the underlying conduction pattern in the phase map (Figure 1D) and the isochrone wave map (Figure 1F). Both isochrone and phase map presented in Figure 1 were manually interpolated to enhance the readability of maps, by combining multiple isochrones to one, if there were >1 isochrone between 2 adjacent electrodes.

To assess the spatial association between PSs and conduction block lines, the distribution of the average Euclidian distances between PSs and the closest site of conduction block was computed. The time segment for comparison between PSs and conduction blocks was chosen as the full lifespan of the PS. Every millisecond when a PS was present, the distance of PSs to the closest block line was determined, and the average distance throughout the lifespan was calculated.

To check for the probability of colocalization of conduction block and PS locations because of chance, we also computed the average minimal distance to conduction block of a random sequence of locations where no PS was detected (named random non-PS location throughout the article) to the closest conduction block, covering the same time interval as the lifespan of each PS. We divided the average distance of PS points and of non-PS locations into 2 subgroups: those that are closer or exactly 1 electrode from the nearest conduction block and those that are farther than 1 electrode to the closest conduction block. The threshold of 1 electrode distance was set to 2 mm to include all block between electrodes in which at least one of the electrodes was adjacent to the PS point. Note that the PS is detected on the intersection of a square of 4 electrodes, and block is detected between pairs of adjacent electrodes.

Simulation Study

We hypothesized that a line of conduction block—even without any turning of the wavefronts—can already lead to PS detections in the phase analysis of the filtered electrograms. To investigate this hypothesis in a more controlled condition, a simple computational model with a line of conduction block separating a virtual medium into a right and a left half was used. The 2-dimensional model we used consisted of a myocyte sheet of 200×500 computational cells coupled diffusively at the interfaces (monodomain conduction model).[32] Tissue electrophysiology was simulated using the Fenton-Karma model.[33] The basic parameters of the Fenton-Karma model reproduce the restitution properties of the Courtemanche-Ramirez-Nattel model of atrial tissue.[34] Details are given in the Data Supplement. A train of 10 consecutive stimulations with a CL of 170 ms on both sides of the line of conduction block was applied. A simulated grid of 16×16 unipolar electrodes was used to reconstruct electrograms, resembling our recording technique during the epicardial mapping study. Unipolar electrograms were computed according to a current source monodomain approximation.[35] The signals were further analyzed to produce isochrone wave maps and phase maps with the same software as the data recorded from human atria in the electrophysiology study.

Statistical Analysis

Results are expressed as means±SD unless otherwise stated. The average minimal distance of a PS during its lifespan to conduction block was compared with the average distance to conduction block of a random sequence of points in the mapping area where no PS was detected within the same time frame. Differences in paired average distances (for every PS and a random sequence of non-PS locations) were tested with the Wilcoxon signed-rank test. Statistical analysis of continuous variables was performed using 2 sample Student t test. P values <0.05 was considered statistically significant.

RESULTS

Phase Singularity Incidence and Lifespan in Phase Mapping

In total, 138 PSs lasting longer than 1 locally measured CL were detected. More PSs were detected in patients

Table. Detailed Distribution of Phase Singularity Per Number of Average CL in Recordings in Patients With Respective P Values Between Groups

	PersAF; Phase Singularity/Cycle (Qty)*	pAF; Phase Singularity/Cycle (Qty)*	P Value
RA	0.09±0.06	0.03±0.03	0.013
LA	0.07±0.05	0.06±0.05	0.58
P value	0.46	0.15	

AF indicates atrial fibrillation; LA, left atrium; pAF, paroxysmal AF; PersAF, persistent AF; and RA, right atrium.

*Phase singularity per number of average CL in recordings in patient was calculated as a total number of phase singularities (count) divided by total duration of the recording (ms), then multiplied by average CL (ms).

with persistent AF than in patients with paroxysmal AF (0.08±0.05 PS/cycle [quantity] in persistent AF group versus 0.04±0.04 PS/cycle in paroxysmal AF, P=0.02). There was no significant difference in PS number between chambers (0.06±0.05 PS/cycle (qty) in left atrial versus 0.06±0.06 PS/cycle in right atrial, P=0.94). A detailed distribution of PS in patients is presented in Table.

The longest PS lifespan was 584 ms, that is, 3.2× the locally measured CL, and the average number of rotations was 1.35. Only 9 of 138 PSs were present for >2 rotations; however, none of them did coincide with the reentrant activations detected by wave mapping. An example of detected PS is shown in Figure 1D.

Direct Comparison of Activation and Phase Mapping

A representative example of a 1:1 comparison between phase map and isochrone wave map is presented in Figure 3A or 3B. Six other examples are presented in Figure 3D and in detail in the Data Supplement. In the isochrone wave maps, a conduction block line is shown as a dashed black-and-white line dividing 2 detected activation waves passing through the mapping area. The PS detected in the phase mapping in Figure 3A was located directly on the conduction block line, located between 2 waves propagating in opposite directions (Figure 3B). When the phase map at the same moment is examined, the map appears to be smoothened, producing a PS at a single point. In Figure 3C, electrograms (top, blue graphs) and phase signals are depicted for the electrodes around the detected PS. As is visible in the recordings from 4 central electrodes, the double potentials appearing on both sides of conduction block (marked green in Figure 3C) modify the processed phase signals such that time point of the phase transition is slightly shifted, and a PS is detected.

Despite the differences presented in Figure 3, the general patterns in both isochrone mapping and the phase mapping were in good agreement. The overall pattern of wavefront propagation was similar—the median time difference between activation time
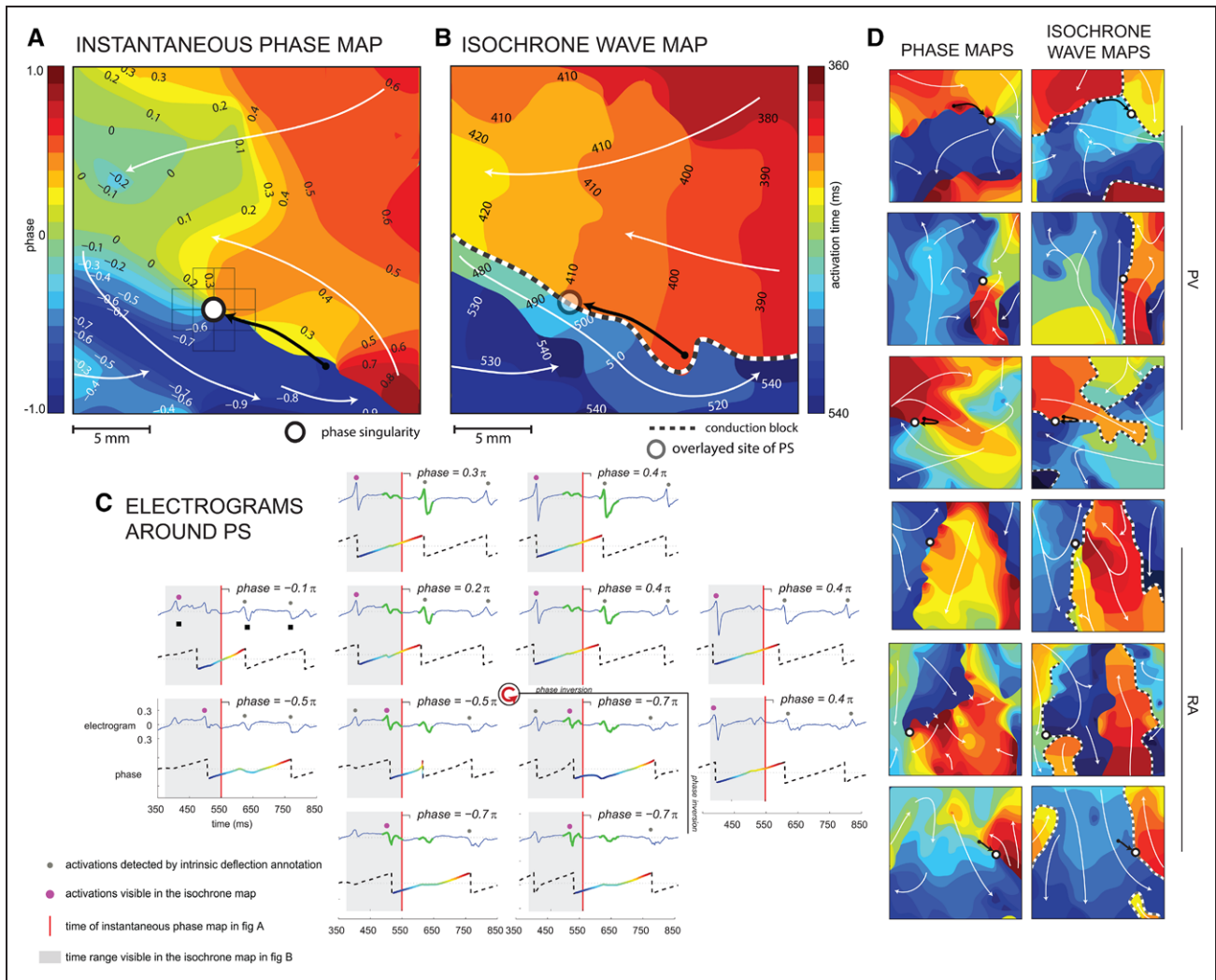
Figure 3. Direct comparison for phase mapping (A) and isochrone wave mapping (B) during detection of a phase singularity (PS) that lasted for 460 ms.

A, Phase map captured at the same time as isochrone wave map in **B**. Phase progresses from $-\pi$ to π and is color-coded with blue corresponding with the beginning of the cycle (wavefront) and dark red with end of the cycle. White circles represent PS locations, small grid corresponds to location of electrodes. **B**, Isochrone wave map prepared from the activations time from earliest (red) to latest (blue) detected in unipolar electrograms. Black and white dashed lines in the isochrones map represent conduction block. White transparent circles superimposed on isochrone wave maps represent PS locations. White arrows indicate the direction of propagation. **C**, Electrograms and phase signals depicted for the electrodes around the detected PS. The red arrow in the middle between graphs represents the location of the depicted PS. Each graph location corresponds to the position of each electrode around the detected PS. Red vertical lines on all the graphs represent the time point for which the phase map is presented. Pink circles mark activation times visible in the isochrone wave map. **D**, Phase and isochrone wave maps for 6 representable detections of a PS in different patients. In all the presented cases the location of the PS coincides with location of conduction block. Black arrows represent the trajectory of PS meandering.

marked by activation time annotation or phase transitions in all recordings was as short as 5.6±2.6 ms. Also, the mean AF CL difference between both methods was negligible (1.58±0.2 ms).

Distance of PSs to Conduction Block Lines

During the lifespan of each PS, the average minimal distance of PSs and random non-PS locations to the closest conduction block line was calculated. One hundred and four out of 138 all PSs detected (74%) were present on average within ≤1 electrode distance from the closest conduction block line (Figure 4A).

One hundred and thirty out of 138 (94%) of PSs appeared within ≤1 electrode distance from the closest conduction block line at some time point during their lifespan. By contrast, only 15% of random non-PS locations were on average within 1 electrode distance from the conduction block (Figure 4B). Importantly, when activation time was annotated manually the same spatial association between PSs and lines of conduction block was found (Section 2.5 in the Data Supplement).

The amount of conduction block events detected in the recording is dependent on the threshold CV_{block} representing minimal acceptable conduction velocity. To
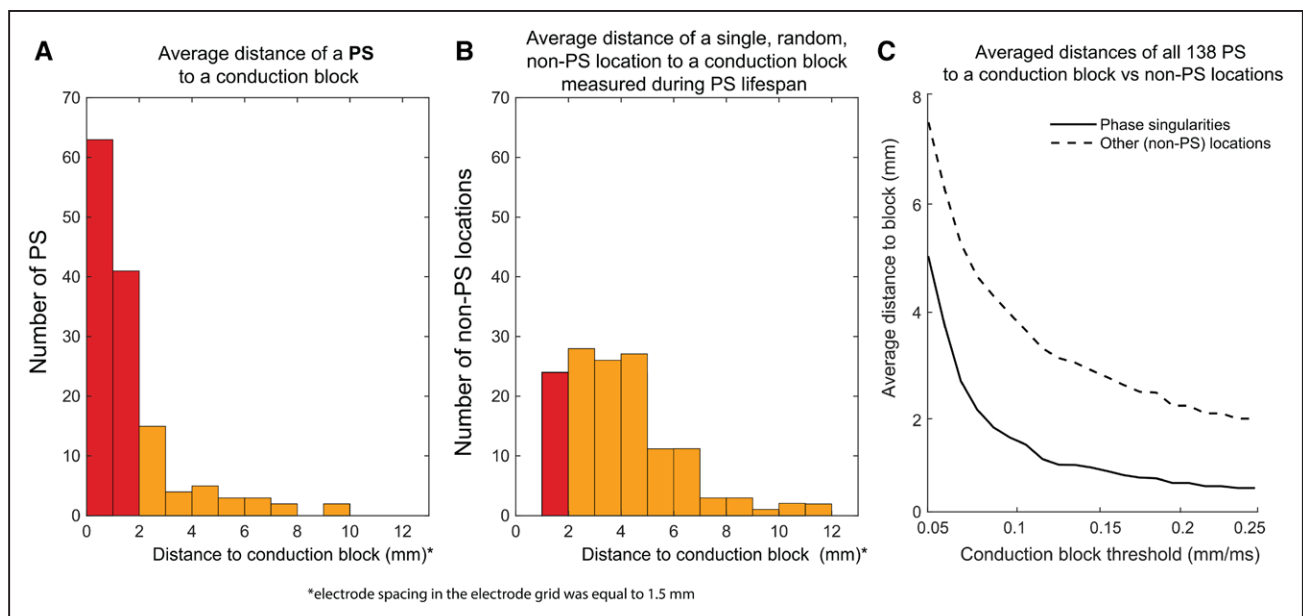
Figure 4. Qualitative analysis of distances of a phase singularity (PS) to conduction block lines.
A, Distribution of average distances of a PS to the closest conduction block line. The distances are averaged over the lifespan of the PS meandered during their lifespan, so their distance to the nearest conduction block may not be constant). **B**, The average distance, during the presence of a PS, of a random sequence of non-PS location to the closest conduction block line. This average is a single value for each of the PSs detected in the study (n=138) depicted in **A**. **C**, Distance of phase singularities to the closest conduction block line as a function of conduction block detection threshold. Solid line presents results for detected PS; dashed curve presents results for the non-PS locations.

test whether the distance of PSs and non-PS locations to the nearest conduction block line depends on the CV_{block}, the averaged distances of all PSs and non-PS locations for different values of CV_{block} are depicted in Figure 4C. With lower thresholds for conduction velocity, the number of detected conduction block events was smaller because waves that conducted more slowly were still treated as normal conduction. However, throughout a large range of thresholds for CV_{block}, PSs were consistently closer to the nearest conduction block compared with non-PS locations.

Influence of Filtering and Phase Calculation Method on the Average Distances Between Conduction Block and Phase Singularity

To investigate how electrogram processing and filtering influence PS detection at the line of conduction block, we compared sinusoidal recomposition with frequency-based filtering.[36] As a substitute of Hilbert transform for phase signal construction, we used time-delay embedding.[28,29] We applied all 4 combinations of electrogram processing to calculate the phase signals. The results of the distribution of average distance of a PS to the nearest conduction block as presented in Figure 4 were calculated with all 4 method combinations and are presented in Figure VII in the Data Supplement. For all tested filtering methods, the PSs were found more than twice as close to conduction block than random non-PS locations (for all

cases the differences in paired average distances resulted in $P<0.001$; tested with a Wilcoxon signed-rank test).

Contribution of Fibrillation Waves to Phase Singularity Formation

Only 8% of all waves detected in all recordings were adjacent to PSs during their lifespan and could be in any way be connected to formation of the PS. Forty-five percent (62) of PSs were formed directly on the conduction block line between 2 waves, propagating in the opposite directions. Twenty-eight percent (39) were formed through interaction of 3 waves that mostly showed sequential activation in the direction of the PS. The full analysis is presented in the Data Supplement. Phase singularity detection had a moderate sensitivity of 77% to detect rotating wavefronts found in activation mapping. The specificity for detection of such rotating waves by PS analysis was only 14 out of 138, that is, around 10%.

In-Silico Comparison of Phase Mapping Versus Activation Mapping

To investigate why PSs appear in the vicinity of a conduction block line, we performed an in-silico study, in which a simple tissue strip divided by a line of complete conduction block was analyzed by isochrone and phase mapping. The results are presented in Figure 5 in the similar fashion as results from experimental study in Figure 3. Double potentials at a line of conduction block
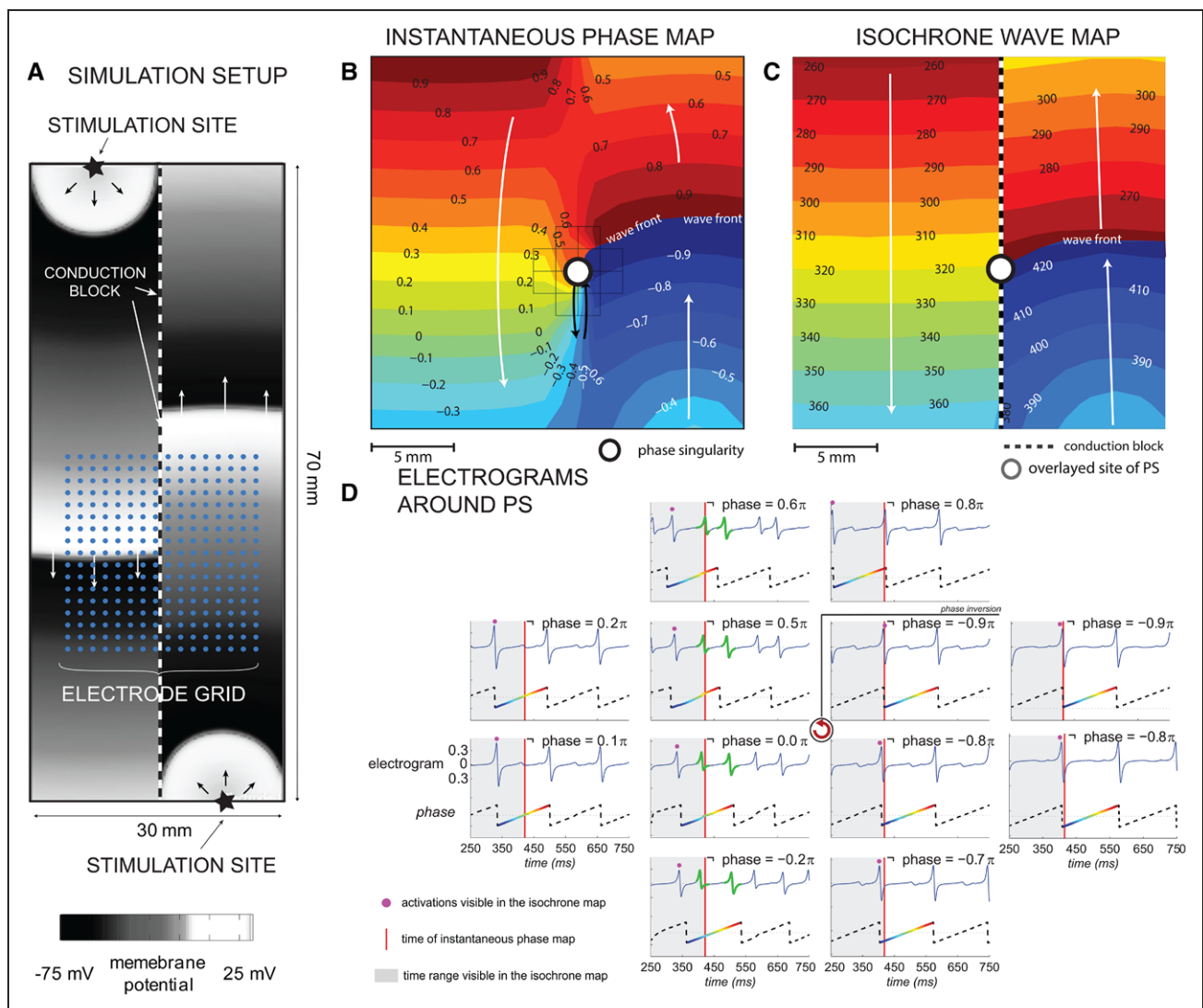
Figure 5. Direct comparison of phase mapping and direct activation mapping in a computer simulation.
A, A simulated tissue strip was divided by a line of conduction block. Consecutive activation fronts propagated in opposite direction on both sides of the conduction block line. Phase map (**B**) and isochrone wave map (**C**) captured at the same time point. **D**, Simulated unipolar electrograms (**top**, blue graphs) and phase signals depicted for the simulated electrodes around the phase singularity (PS). At the conduction block line, filtering of the double potentials (green color) shifted the time of phase inversion for some of the electrodes. The resulting smoothening effect on phase near the conduction block produces an artificial PS at the conduction block line.

DISCUSSION

Defining the pattern of activation during AF is fundamental to our understanding of the pathophysiology of AF. The current diversity in the perception of different mechanisms sustaining AF is partly because of the fact that a large diversity of AF mapping technologies is used by investigators studying AF mechanisms. Furthermore, no consensus has been achieved so far with regards to minimal requirements for electrogram recordings and analysis, as well as interpretation of AF electrograms. Recent phase mapping studies have identified rotors as drivers for AF[11,12] but are inconsistent with direct-contact mapping studies in patients with AF[9,37] and differ largely with regard to the spatiotemporal stationarity of rotors.[11,12] This raises significant conceptual questions about the existence of these drivers for AF but also about the role of signal processing in the interpretation of fibrillation electrograms. Here, we aim to clarify the role of electrogram filtering and phase analysis in the identification of rotating fibrillation waves.

(marked by green color in Figure 3D) were blurred by the filtering step, affecting reconstructed electrogram's phase for some of these electrodes (bottom curves in plots). This resulted in a smoothing effect on the spatial image of phase near the line of conduction block and produced an artificial PS located at the conduction block line.

Our results imply that the identification of PSs using phase analysis of filtered electrograms has a very low specificity in identifying wavefronts rotating >360 degrees as identified by isochrone wave maps. Instead, PSs to a large extent reflect lines of conduction block located between nonrotating wavefronts.

Characteristics of PSs as Markers for Rotors

We evaluated 2 approaches of interpretation of atrial electrogram recordings, one based on detecting activation times and the other based on phase mapping. We found that a high number of detected PSs were located very close to a line of conduction block at the exact same time point. Moreover, in a simple in-silico study, we observed that a block line is a sufficient condition to result in PS detection during phase mapping. More specifically, conduction of 2 waves in opposite directions on both sides of a line of conduction block may become represented as a rotating pattern in phase analysis. This is likely because of a shift of the phase inversion in time from the time of true tissue activation caused by the required filtering step of the electrograms.

Our results suggest that using phase analysis on complex electrograms recorded during AF may not be specific enough to mark true rotational activity. Instead, repetitive conduction patterns along a line of conduction block could produce an apparent PS and may be misinterpreted as a rotor. Repetitive conduction patterns along a conduction block which are consistent with other studies showing spatiotemporal linking of waves[38] may result in detection of rotors of considerable live spans in phase analysis.

Our results certainly do not imply that rotating waves do not exist. In fact, using our activation time annotation and isochrone wave map algorithms, we could identify 18 waves that rotated >360 degrees within the mapping area. This confirms our previous observations[23] that during human AF recorded from the epicardial surface such waves are a rare phenomenon (in this study about 0.2% of all waves). Fourteen out of these rotating 18 waves (waves rotating >360 degrees) were adjacent to a PS location at least during some time in their lifespan. Thus, the sensitivity of phase analysis to detect rotating waves confirmed by activation time annotation was moderate (77%). However, a much more relevant result of our study is that the specificity of phase mapping to detect rotating waves was as low as 10% (only 14 out of 138 detected PSs actually represented rotating waves).

Filtering of Atrial Signals

Analysis of AF activation patterns always requires various degrees of signal preprocessing, such as filtering of initially recorded electrograms. Both techniques that showed rotors to be drivers of AF—ECG-I and FIRM basket mapping—use phase analysis to determine and analyze conduction behavior during AF. The discrepancy between conduction patterns shown by phase analysis and direct activation time mapping in this study shows how much filtering changes our perception of the conduction pattern during AF. The effect of annotation and phase mapping was also reported recently by Zaman et al[39] where only 5 of 25 rotor and focal sources shown by phase mapping could be confirmed identified on isochrone maps calculated from annotated electrograms from the same FIRM basket catheters recordings.

In our study, applying 2 different filtering techniques with 2 different phase reconstruction methods led to detection of PSs preferentially on the line of conduction block, suggesting that the PSs are the result of sequential activation of wavefronts near the line of conduction block rather than because of truly rotational activation. Visual inspection confirmed that the dominant pattern underlying the PS was conduction of 2 waves in opposite directions on both sides of a line of conduction block.

Fibrillatory patterns mapped with phase analysis techniques both in ECG-I[10] and FIRM[12,19] show rather simple, smooth conduction pattern, that is, higher spatial organization and much lower complexity than methods based on annotation of local unipolar electrograms. In ECG-I this may be, at least partially, because of a filtering effect of the thorax as volume conductor and related limitations of the inverse solution performed to compute electrograms on the atrial surface. In case of contact electrograms used in FIRM mapping, this is likely to be an effect of limited resolution of the grid (increasing the likelihood that a block line is present between adjacent electrodes), limited contact, and the processing algorithms applied to compute phase maps.

Apart from the temporal filtering performed during signal preprocessing, one can consider spatial filtering of the detection of activation wavefronts. Previous work by our group[23] demonstrated that increasing electrode spacing heavily influences the number of detected PSs. Increasing electrode spacing represents a form of low-frequency spatial filtering of the signal. Our data demonstrate that low-frequency spatial filtering of phases can create a bias toward detection of rotors.

Clinical and Physiological Implications

If our hypothesis is correct and if PSs are indeed markers for conduction block lines separating nonrotating waves rather than a reliable method to detect rotating wavefronts, several surprising results reported in recent AF mapping studies can be explained more easily.

For example, published videos depicting detected rotors in other studies (eg, see[12]) show apparent discontinuous conduction near detected PSs, a pattern usually not associated with rotors. These areas may indicate an area of conduction slowing or conduction block near detected phase singularity, affecting the detected pattern. In line with this hypothesis, Vijayakumar et al[40] presented an ECG-I study in patients with atrial flutter or ventricular tachycardia comparing activation time maps with phase maps and also found examples of sequential activation around a line of conduction block being detected as PSs in the phase mapping approach.

Furthermore, in another study involving noninvasive mapping of atrial electrical activity, Haissaguerre et al[41] reported that the reentrant and focal sources detected in phase mapping appeared at the borders of fibrotic atrial regions, identified by magnetic resonance imaging atrial imaging.[42] In such fibrotic atrial regions, the probability of conduction block is high.[43,44] The colocalization between rotors and fibrotic areas may actually reflect the high incidence of block events close to fibrotic regions.

Finally, our results could offer an explanation for the counterintuitive notion that ablation at the core of rotors can sometimes terminate AF. The probability density maps produced by the ECG-I approach by Haissaguerre et al[41] might reflect areas with a higher probability of conduction block and not necessarily areas where truly rotating wavefronts appear. Such areas of a higher probability of conduction block could contribute to wave generation and increase AF complexity. When eliminated by ablation, AF complexity may decline, and AF may eventually terminate.

Furthermore, our results suggest that the rotors detected by FIRM used to analyze endocardial electrograms could reflect spatially constant lines of block in the endocardial conduction pattern. Recently Li et al[45] and Hansen et al[46] demonstrated that in Langendorff-perfused human atria AF can be driven by localized stationary reentrant circuits along loops of endocardial trabeculae. The gap between the endocardial bundles represents an anatomic line of block which in phase mapping may be detected as PSs. Whether localized and stationary reentry circuits as described by Hansen et al[46] reflect rotors identified by FIRM certainly warrants further investigation.

Limitations

In our study, we found only short-lasting PSs; the longest recorded lifespan was 584 ms (3.2 rotations). This may not fully reflect the conduction pattern on the endocardial side of the atrial wall. However, similar findings with respect to the lifespan of PSs were reported in a study by Haissaguerre et al[11] exploring the use of body surface potential mapping and inverse solution (ECG-I approach) to identify rotors in the atria.

Methods for determining local atrial activation using unipolar electrograms in AF are limited by absence of a gold standard and the inherent complexities of the electrograms. Thus, there may be limitations to conclusions drawn from activation mapping in AF.

Moreover, we have not validated the existence of conduction block. Future studies using techniques such as extension of a line of conduction by creating an ablation line to an anatomic boundary might further validate the conduction lines identified using activation mapping.

The field of view we obtained during high-density epicardial mapping was a 2.4×2.4 cm. This is just a portion of the entire atrial surface and using this technique a full view on all rotational activity in the atria cannot be achieved. However, there are 3 aspects of our epicardial mapping approach that strengthen our conclusions: (1) we used high-density mapping grids which provide more reliable analysis of conduction patterns than the often sparse set of points obtained using basket catheters, (2) the majority (101 out of 138) of PSs we found originated and disappeared within field of view suggesting that our conclusion regarding the short lifespan of PSs is reliable, (3) we mapped an area between pulmonary veins, which is often reported[12] as a frequent location of stable PSs. Yet, even in this area, PSs were short-lived and true rotation occurred in <1% of all fibrillation waves.

This study was performed in patients undergoing cardiac surgery and might not apply to other patients with AF.

As the techniques of contact mapping, FIRM and ECG-I differ substantially (epicardial or endocardial measurement, density of coverage, etc), the rotating wavefronts presented in our study may represent different phenomena than the rotational activity reported by ECG-I and FIRM-based studies.

Conclusions

Rotors identified by phase analysis of filtered, epicardial atrial electrograms are more likely to reflect lines of conduction block between nonrotating waves than rotating wavefronts. A single line of block is sufficient to produce a PS when phase analysis is used on filtered electrograms from that area. Our study raises fundamental questions about the very use of phase analysis to unravel the pathophysiology of AF and to identify rotors as targets for AF ablation. However, absence of a gold standard for the analysis of local atrial activation in AF may limit these conclusions.

Correspondence

Ulrich Schotten, MD, PhD, Department. of Physiology, Cardiovascular Research Institute Maastricht, PO Box 616, 6200MD Maastricht, the Netherlands. Email schotten@maastrichtuniversity.nl

Affiliations

Department of Physiology, Maastricht University, the Netherlands (P.P., S.Z., A.v.H., S.V.). Cardiovascular Research Institute Maastricht (CARIM), the Netherlands (P.P., S.Z., A.v.H., B.M., J.M., H.J.C., S.V., U.S.). Department of Cardiology, Electrophysiology, University Medical Center Hamburg-Eppendorf, Germany (P.K.). Department of Cardiothoracic Surgery (B.M., J.M.) and Department of Cardiology (H.J.C.), Maastricht University Medical Center, the Netherlands.

Disclosures

Dr Schotten received consultancy fees or honoraria from the Università della Svizzera Italiana (USI, Switzerland, significant), the Universities of Utah and California (modest), Roche Diagnostics (Switzerland, modest), Bayer Healthcare (Germany, modest). He is also cofounder, scientific director, and shareholder of YourRhythmics BV, a spin-off company of the University Maastricht (significant). Dr Kuklik received lecture fees from Abbott, Inc (modest). The other authors report no conflicts.

REFERENCES

1. Andrade J, Khairy P, Dobrev D, Nattel S. The clinical profile and pathophysiology of atrial fibrillation: relationships among clinical features, epidemiology, and mechanisms. *Circ Res*. 2014;114:1453–1468. doi: 10.1161/CIRCRESAHA.114.303211
2. Wokhlu A, Hodge DO, Monahan KH, Asirvatham SJ, Friedman PA, Munger TM, Cha YM, Shen WK, Brady PA, Bluhm CM, Haroldson JM, Hammill SC, Packer DL. Long-term outcome of atrial fibrillation ablation: impact and predictors of very late recurrence. *J Cardiovasc Electrophysiol*. 2010;21:1071–1078. doi: 10.1111/j.1540-8167.2010.01786.x
3. Schotten U, Dobrev D, Platonov PG, Kottkamp H, Hindricks G. Current controversies in determining the main mechanisms of atrial fibrillation. *J Intern Med*. 2016;279:428–438. doi: 10.1111/joim.12492
4. Heijman J, Voigt N, Nattel S, Dobrev D. Cellular and molecular electrophysiology of atrial fibrillation initiation, maintenance, and progression. *Circ Res*. 2014;114:1483–1499. doi: 10.1161/CIRCRESAHA.114.302226
5. Allessie M, de Groot N. CrossTalk opposing view: rotors have not been demonstrated to be the drivers of atrial fibrillation. *J Physiol*. 2014;592:3167–3170. doi: 10.1113/jphysiol.2014.271809
6. Moe GK, Rheinboldt WC, Abildskov JA. A computer model of atrial fibrillation. *Am Heart J*. 1964;67:200–220.
7. Konings KT, Kirchhof CJ, Smeets JR, Wellens HJ, Penn OC, Allessie MA. High-density mapping of electrically induced atrial fibrillation in humans. *Circulation*. 1994;89:1665–1680.
8. Lee G, Kumar S, Teh A, Madry A, Spence S, Larobina M, Goldblatt J, Brown R, Atkinson V, Moten S, Morton JB, Sanders P, Kistler PM, Kalman JM. Epicardial wave mapping in human long-lasting persistent atrial fibrillation: transient rotational circuits, complex wavefronts, and disorganized activity. *Eur Heart J*. 2014;35:86–97. doi: 10.1093/eurheartj/eht267
9. Allessie MA, de Groot NM, Houben RP, Schotten U, Boersma E, Smeets JL, Crijns HJ. Electropathological substrate of long-standing persistent atrial fibrillation in patients with structural heart disease: longitudinal dissociation. *Circ Arrhythm Electrophysiol*. 2010;3:606–615. doi: 10.1161/CIRCEP.109.910125

10. Cuculich PS, Wang Y, Lindsay BD, Faddis MN, Schuessler RB, Damiano RJ Jr, Li L, Rudy Y. Noninvasive characterization of epicardial activation in humans with diverse atrial fibrillation patterns. *Circulation*. 2010;122:1364–1372. doi: 10.1161/CIRCULATIONAHA.110.945709
11. Haissaguerre M, Hocini M, Denis A, Shah AJ, Komatsu Y, Yamashita S, Daly M, Amraoui S, Zellerhoff S, Picat MQ, Quotb A, Jesel L, Lim H, Ploux S, Bordachar P, Attuel G, Meillet V, Ritter P, Derval N, Sacher F, Bernus O, Cochet H, Jais P, Dubois R. Driver domains in persistent atrial fibrillation. *Circulation*. 2014;130:530–538. doi: 10.1161/CIRCULATIONAHA.113.005421
12. Narayan SM, Krummen DE, Shivkumar K, Clopton P, Rappel WJ, Miller JM. Treatment of atrial fibrillation by the ablation of localized sources: CONFIRM (Conventional Ablation for Atrial Fibrillation with or Without Focal Impulse and Rotor Modulation) trial. *J Am Coll Cardiol*. 2012;60:628–636. doi: 10.1016/j.jacc.2012.05.022
13. Miller JM, Kowal RC, Swarup V, Daubert JP, Daoud EG, Day JD, Ellenbogen KA, Hummel JD, Baykaner T, Krummen DE, Narayan SM, Reddy VY, Shivkumar K, Steinberg JS, Wheelan KR. Initial independent outcomes from focal impulse and rotor modulation ablation for atrial fibrillation: multicenter FIRM registry. *J Cardiovasc Electrophysiol*. 2014;25:921–929. doi: 10.1111/jce.12474
14. Narayan SM, Baykaner T, Clopton P, Schricker A, Lalani GG, Krummen DE, Shivkumar K, Miller JM. Ablation of rotor and focal sources reduces late recurrence of atrial fibrillation compared with trigger ablation alone: extended follow-up of the CONFIRM trial (Conventional Ablation for Atrial Fibrillation With or Without Focal Impulse and Rotor Modulation). *J Am Coll Cardiol*. 2014;63:1761–1768. doi: 10.1016/j.jacc.2014.02.543
15. Ramirez FD, Birnie DH, Nair GM, Szczotka A, Redpath CJ, Sadek MM, Nery PB. Efficacy and safety of driver-guided catheter ablation for atrial fibrillation: a systematic review and meta-analysis. *J Cardiovasc Electrophysiol*. 2017;28:1371–1378. doi: 10.1111/jce.13313
16. Mohanty S, Mohanty P, Trivedi C, Gianni C, Della Rocca DG, Di Biase L, Natale A. Long-term outcome of pulmonary vein isolation with and without focal impulse and rotor modulation mapping. *Circ Arrhythmia Electrophysiol*. 2018;11:e005789. doi: 10.1161/CIRCEP.117.005789
17. Baykaner T, Rogers AJ, Meckler GL, Zaman J, Navara R, Rodrigo M, Alhusseini M, Kowalewski CAB, Viswanathan MN, Narayan SM, Clopton P, Wang PJ, Heidenreich PA. Clinical implications of ablation of drivers for atrial fibrillation: a systematic review and meta-analysis. *Circ Arrhythm Electrophysiol*. 2018;11:e006119. doi: 10.1161/CIRCEP.117.006119
18. Zeemering S, Maesen B, Nijs J, Lau DH, Granier M, Verheule S, Schotten U. Automated quantification of atrial fibrillation complexity by probabilistic electrogram analysis and fibrillation wave reconstruction. *Conf Proc IEEE Eng Med Biol Soc*. 2012;2012:6357–6360. doi: 10.1109/EMBC.2012.6347448
19. Narayan SM, Zaman JAB. Mechanistically based mapping of human cardiac fibrillation. *J Physiol*. 2016;594:2399–2415. doi: 10.1113/JP270513
20. Kuklik P, Zeemering S, Maesen B, Maessen J, Crijns HJ, Verheule S, Ganesan AN, Schotten U. Reconstruction of instantaneous phase of unipolar atrial contact electrogram using a concept of sinusoidal recomposition and Hilbert transform. *IEEE Trans Biomed Eng*. 2015;62:296–302. doi: 10.1109/TBME.2014.2350029
21. Umapathy K, Nair K, Masse S, Krishnan S, Rogers J, Nash MP, Nanthakumar K. Phase mapping of cardiac fibrillation. *Circ Arrhythm Electrophysiol*. 2010;3:105–114. doi: 10.1161/CIRCEP.110.853804
22. Eckstein J, Zeemering S, Linz D, Maesen B, Verheule S, van Hunnik A, Crijns H, Allessie MA, Schotten U. Transmural conduction is the predominant mechanism of breakthrough during atrial fibrillation: evidence from simultaneous endo-epicardial high-density activation mapping. *Circ Arrhythm Electrophysiol*. 2013;6:334–341. doi: 10.1161/CIRCEP.113.000342
23. Kuklik P, Zeemering S, van Hunnik A, Maesen B, Pison L, Lau DH, Maessen J, Podziemski P, Meyer C, Schaffer B, Crijns H, Willems S, Schotten U. Identification of rotors during human atrial fibrillation using contact mapping and phase singularity detection: technical considerations. *IEEE Trans Biomed Eng*. 2017;64:310–318. doi: 10.1109/TBME.2016.2554660
24. Roney CH, Cantwell CD, Qureshi NA, Chowdhury RA, Dupont E, Lim PB, Vigmond EJ, Tweedy JH, Ng FS, Peters NS. Rotor tracking using phase of electrograms recorded during atrial fibrillation. *Ann Biomed Eng*. 2017;45:910–923. doi: 10.1007/s10439-016-1766-4
25. Everett TH IV, Kok LC, Vaughn RH, Moorman JR, Haines DE. Frequency domain algorithm for quantifying atrial fibrillation organization to increase defibrillation efficacy. *IEEE Trans Biomed Eng*. 2001;48:969–978.
26. Traykov VB, Pap R, Saghy L. Frequency domain mapping of atrial fibrillation - methodology, experimental data and clinical implications. *Curr Cardiol Rev*. 2012;8:231–238.

27. Botteron GW, Smith JM. Quantitative assessment of the spatial organization of atrial fibrillation in the intact human heart. *Circulation*. 1996;93:513 LP–518 LP.

28. Gray RA, Pertsov AM, Jalife J. Spatial and temporal organization during cardiac fibrillation. *Nature*. 1998;392:75–78. doi: 10.1038/32164

29. Bray MA, Wikswo JP. Considerations in phase plane analysis for nonstationary reentrant cardiac behavior. *Phys Rev E Stat Nonlin Soft Matter Phys*. 2002;65(5 pt 1):051902. doi: 10.1103/PhysRevE.65.051902

30. Bray MA, Lin SF, Aliev RR, Roth BJ, Wikswo JP Jr. Experimental and theoretical analysis of phase singularity dynamics in cardiac tissue. *J Cardiovasc Electrophysiol*. 2001;12:716–722.

31. Eason JC, Trayanova NA. Phase singularities and termination of spiral wave reentry. *Annu Reports Res React Institute, Kyoto Univ*. 2001;1:66–69.

32. Podziemski P, Zebrowski JJ. A simple model of the right atrium of the human heart with the sinoatrial and atrioventricular nodes included. *J Clin Monit Comput*. 2013;27:481–498. doi: 10.1007/s10877-013-9429-6

33. Fenton F, Karma A. Vortex dynamics in three-dimensional continuous myocardium with fiber rotation: filament instability and fibrillation. *Chaos*. 1998;8:20–47. doi: 10.1063/1.166311

34. Oliver RA, Krassowska W. Reproducing cardiac restitution properties using the Fenton-Karma membrane model. *Ann Biomed Eng*. 2005;33: 907–911.

35. Jacquemet V. *A Biophysical Model of Atrial Fibrillation and Electrograms: Formulation, Validation and Applications* [dissertation]. Lausanne Switzerland: École polytechnique fédérale de Lausanne; Thése no:2996; 2004.

36. Roney CH, Cantwell CD, Qureshi NA, Chowdhury RA, Dupont E, Lim PB, Vigmond EJ, Tweedy JH, Ng FS, Peters NS. Rotor tracking using phase of electrograms recorded during atrial fibrillation. *Ann Biomed Eng*. 2017;45:910–923. doi: 10.1007/s10439-016-1766-4

37. Lee S, Sahadevan J, Khrestian CM, Cakulev I, Markowitz A, Waldo AL. Simultaneous biatrial high-density (510-512 electrodes) epicardial mapping of persistent and long-standing persistent atrial fibrillation in patients: new insights into the mechanism of its maintenance. *Circulation*. 2015;132:2108–2117. doi: 10.1161/CIRCULATIONAHA.115.017007

38. Gerstenfeld EP, Sahakian a V, Swiryn S. Evidence for transient linking of atrial excitation during atrial fibrillation in humans. *Circulation*. 1992;86:375–82.

39. Zaman JA, Lalani GG, Baykaner T, Park S, Krummen DE, Wang PJ, Narayan SM. Phase analysis detects human atrial fibrillation sources while classical activation mapping may not: reconciling classical and computational mapping [abstract 18492]. *Circulation*. 2015;132:A18492 LP–A18492 LP.

40. Vijayakumar R, Vasireddi SK, Cuculich PS, Faddis MN, Rudy Y. Methodology considerations in phase mapping of human cardiac arrhythmias. *Circ Arrhythmia Electrophysiol*. 2016;9:e004409. doi: 10.1161/CIRCEP.116.004409

41. Haissaguerre M, Shah AJ, Cochet H, Hocini M, Dubois R, Vigmond E, Bernus O, Trayanova N. Intermittent drivers anchoring to structural heterogenei- ties as a major pathophysiologic mechanism of human persistent atrial fibrillation. *J Physiol*. 2016;594:2387–2398. doi: 10.1113/JP270617

42. Vigmond E, Pashaei A, Cochet H, Amroui S, Haissaguerre M. Percolation as a mechanism to explain atrial fractionated electrograms and reentry in a fibrosis model based on imaging data. *Hear Rhythm*. 2016;13:1536–1543. doi: 10.1016/j.hrthm.2016.03.019

43. Allessie M, Ausma J, Schotten U. Electrical, contractile and structural remodeling during atrial fibrillation. *Cardiovasc Res*. 2002;54:230–246.

44. Sánchez-Quintana D, López-Mínguez JR, Pizarro G, Murillo M, Cabrera JA. Triggers and anatomical substrates in the genesis and perpetuation of atrial fibrillation. *Curr Cardiol Rev*. 2012;8:310–326. doi: 10.2174/157340312803760721

45. Li N, Csepe TA, Hansen BJ, Sul LV, Kalyanasundaram A, Zakharkin SO, Zhao J, Guha A, Van Wagoner DR, Kilic A, Mohler PJ, Janssen PM, Biesiadecki BJ, Hummel JD, Weiss R, Fedorov VV. Adenosine-induced atrial fibrillation: localized reentrant drivers in lateral right atria because of heterogeneous expression of adenosine A1 receptors and GIRK4 subunits in the human heart. *Circulation*. 2016;134:486–498. doi: 10.1161/CIRCULATIONAHA.115.021165

46. Hansen BJ, Zhao J, Csepe TA, Moore BT, Li N, Jayne LA, Kalyanasundaram A, Lim P, Bratasz A, Powell KA, Simonetti OP, Higgins RS, Kilic A, Mohler PJ, Janssen PM, Weiss R, Hummel JD, Fedorov VV. Atrial fibrillation driven by micro-anatomic intramural re-entry revealed by simultaneous sub-epicardial and sub-endocardial optical mapping in explanted human hearts. *Eur Heart J*. 2015;36:2390–2401. doi: 10.1093/eurheartj/ehv233